Phase transitions in a generalized $|\psi|^4$ model

Wolfhard Janke and Elmar Bittner

Institut für Theoretische Physik, Universität Leipzig,
Augustusplatz 10/11, D-04109 Leipzig, Germany

Monte Carlo simulations are employed for studying a generalized three-dimensional complex $|\psi|^4$ field theory with an additional fugacity term controlling the vortex-line density. It is shown that only with such an extra term, the XY type second-order phase transitions of the standard model can be tuned in certain regions of the phase diagram to become first-order. In particular, this settles a recent controversy in the standard model related to the measure of the functional integral. Also the topological excitations of the model (vortex networks) are carefully examined.

PACS: 02.70.Lq, 64.60.-i
Key words: phase transitions, 3D XY model universality class, vortex networks

1 Introduction

The Ginzburg–Landau or $|\psi|^4$ field theory is the paradigmatic model for studying critical phenomena using field-theoretic techniques [1]. Perturbative calculations of critical exponents and amplitude ratios of the Ising ($n = 1$), XY ($n = 2$), Heisenberg ($n = 3$) and other O(n) spin models relied heavily on this field-theoretic formulation [2]. Even though the spin models contain only directional fluctuations, while for n-component Ginzburg–Landau fields with $n \geq 2$ directional and size fluctuations seem to be equally important, the two descriptions are completely equivalent, as is expected through the concept of universality and has been proved explicitly for superfluids with $n = 2$, where the spin model reduces to an XY model [3]. Therefore it appeared as a surprise when, on the basis of an approximate variational approach to the two-component Ginzburg–Landau model, Curty and Beck [4] recently predicted for certain parameter ranges the possibility of first-order phase transitions induced by phase fluctuations which subsequently were apparently confirmed numerically [5–8].

We therefore performed an independent Monte Carlo study of the standard three-dimensional Ginzburg–Landau model [9]. Contrary to the previous numerical findings, our results clearly support the prevailing opinion that the nature of the transition is of second (or higher) order, and the source for this numerical disagreement could be pinpointed [9]. Here we review a recent generalization of the standard model by adding a fugacity term which implicitly controls the vortex-line density of the model [10]. By means of this extra term it is indeed possible to tune the generalized system into a region with first-order phase transitions.

The layout of the remainder of this paper is organized as follows. In Sec. 2 we first recall the standard model, and then discuss its generalization and the observables used to map out its phase diagram. Next we describe in Sec. 3 the simulation techniques employed in our extensive Monte Carlo study of the generalized model.

The results of our simulations are presented in Sec. 4, and in Sec. 5 we conclude with a summary of our main findings.

2 The generalized $|\psi|^4$ model

We start from the standard complex or two-component Ginzburg–Landau field theory defined by the Hamiltonian

$$H[\psi] = \int \mathrm{d}^d r \left[\alpha |\psi|^2 + \frac{b}{2} |\psi|^4 + \frac{\gamma}{2} |\nabla \psi|^2 \right], \quad \gamma > 0 \,, \tag{1}$$

where $\psi(\vec{r}) = \psi_x(\vec{r}) + \mathrm{i}\psi_y(\vec{r}) = |\psi(\vec{r})| \mathrm{e}^{\mathrm{i}\phi(\vec{r})}$ is a complex field, and α, b, and γ are temperature independent coefficients derived from a microscopic model. In order to carry out Monte Carlo simulations we put the model (1) on a d-dimensional hypercubic lattice with spacing a. Adopting the notation of Ref. [4], we introduce rescaled fields $\tilde{\psi} = \psi / \sqrt{|\alpha|/b}$ and $\vec{u} = \vec{r}/\xi$, where $\xi = \sqrt{\gamma/|\alpha|}$ is the mean-field correlation length at zero temperature. Only two independent parameters remain,

$$\tilde{V}_0 = \frac{1}{k_B} \frac{|\alpha|}{b} \gamma a^{d-2} \,, \quad \tilde{\sigma} = \frac{a^2}{\xi^2} \,,$$

where $\tilde{V}_0$ merely sets the temperature scale and can thus be absorbed in the definition of the reduced temperature. After these rescalings the partition function actually considered is then given by

$$Z = \int D\psi D\bar{\psi} \, \mathrm{e}^{-H/T} \tag{2}$$

with

$$H[\psi] = \sum_{n=1}^{N} \left[\frac{\sigma}{2} \left(|\psi_n|^2 - 1 \right)^2 + \frac{1}{2} \sum_{\mu=1}^{d} |\psi_n - \psi_{n+\mu}|^2 \right], \tag{3}$$

where $\int D\psi \, D\bar{\psi} \equiv \int D \operatorname{Re}\psi \, D \operatorname{Im}\psi$ stands short for integrating over all possible complex field configurations, μ denotes the unit vectors along the d coordinate axes, and $N = L^d$ is the total number of sites.

Using the same parametrization, Curty and Beck [4] approximated this partition function by integrating only over the phase. In a mean-field type treatment they dropped the integration over $R_n = |\psi_n|$ and determined the minimum of the free energy with respect to R. Assuming that the gradient of the amplitude is zero, this leads to the equation

$$\sigma(R^2 + R^4) - \tfrac{1}{2} T + R^2 f(K) = 0 \,, \tag{4}$$

where $f(K) = \langle f_n \rangle$ is the numerically determined expectation value within the XY spin model of $f_n = \sum_{\mu=1}^{d} \left[1 - \cos(\phi_n - \phi_{n+\mu}) \right]$ with a dimensionless coupling constant (inverse temperature) $K = R^2/T$. By looking at the graphical solution

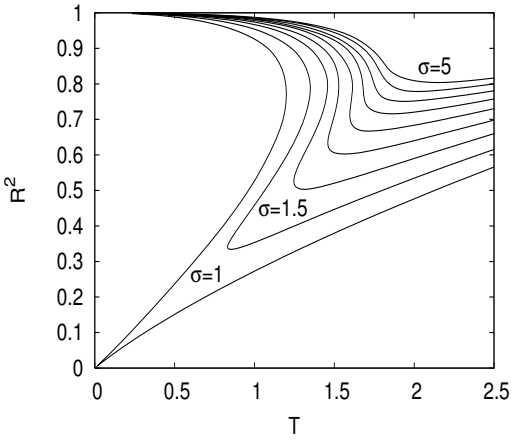

Fig. 1. Graphical solution of the mean-field type equation (4), indicating metastabilities for small σ and hence the appearance of first-order phase transitions.

sketched in Fig. 1 it is evident from the double valued shape of R^2 that metastabilities develop for small σ, predicting a first-order phase transition in this parameter region.

In several papers [5–8] this quasi-analytical prediction was tested by Monte Carlo simulations and, as the main result, apparently confirmed numerically. If true, these findings would have an enormous impact on the theoretical description of many related systems such as superfluid helium, superconductors, certain liquid crystals and possibly even the electroweak standard model of elementary particle physics [11,12]. We have therefore performed independent Monte Carlo simulations of the model (2), (3) to test whether the possibility of a phase-fluctuation induced first-order transition is a real effect or not [9]. Our results, however, clearly support the prevailing opinion that the nature of the transition is of second (respectively higher) order for all values of σ.

What is the source for this disagreement? In Ref. [9] we have demonstrated that it is caused by an incorrect sampling of the Jacobian which emerges from the complex measure in (2) when transforming the field representation to polar coordinates, $\psi_n = R_n \mathrm{e}^{\mathrm{i}\phi_n}$. When updating in the simulations the modulus $R_n = |\psi_n|$ and the angle ϕ_n, one has to rewrite the functional measure of the partition function (2) as

$$D\psi D\bar{\psi} = R\, DR\, D\phi\,, \tag{5}$$

where $DR \equiv \prod_{n=1}^{N} \mathrm{d}R_n$ and $R \equiv \prod_{n=1}^{N} R_n$ is the Jacobian of this transformation. The Jacobian factor may be easily missed when coding Metropolis update proposals for the modulus and angle in a Monte Carlo simulation program. While for the angles it is correct to use update proposals of the form $\phi_n \to \phi_n + \delta\phi_n$ with $-\Delta\phi \leq \delta\phi_n \leq \Delta\phi$ (where $\Delta\phi$ is chosen such as to assure an optimal acceptance ratio), the similar procedure for the modulus, $R_n \to R_n + \delta R_n$ with $-\Delta R \leq \delta R_n \leq \Delta R$, would

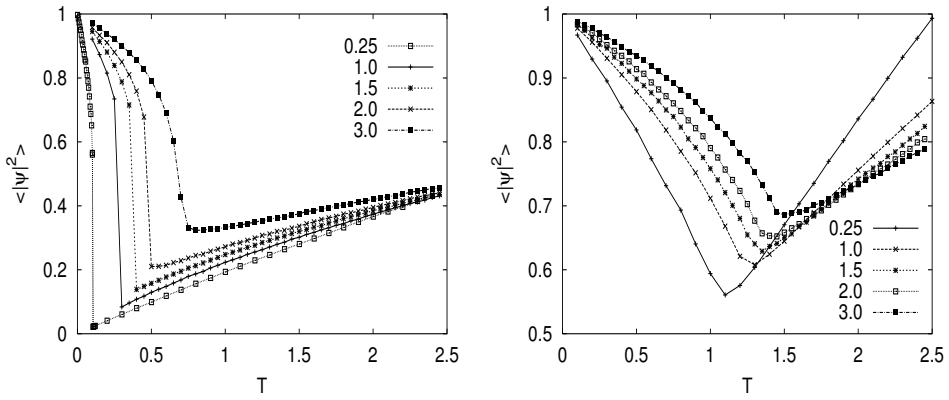

Fig. 2. Mean-square amplitude $\langle|\psi|^2\rangle$ of the three-dimensional complex Ginzburg–Landau model on a 15^3 cubic lattice for $\sigma = 0.25, \ldots, 3.0$ when erroneously omitting the Jacobian factor R of the functional measure (5) (left), corresponding to $\kappa = 0$ in the generalized model (7), and in the standard formulation with the proper functional measure (right), corresponding to $\kappa = 1$.

be incorrect since this ignores the R_n factor coming from the Jacobian. In fact, if we purposely ignore the Jacobian and simulate the model (2), (3) (erroneously) without the R-factor, then we obtain a completely different behavior than in the correct case, cf. Fig. 2. These results reproduce[1]) those in Refs. [5] and [8], and from this data one would indeed conclude evidence for a first-order phase transition when σ is small. With the correct measure, on the other hand, we find *no* first-order signal down to $\sigma = 0.01$.

To treat the measure in Eq. (5) properly one can either use the identity $R_n \mathrm{d}R_n = \frac{1}{2}\,\mathrm{d}R_n^2$ and update the squared moduli $R_n^2 = |\psi_n|^2$ according to a uniform measure (where the update proposal $R_n^2 \to R_n^2 + \delta_n$ with $-\Delta \le \delta_n \le \Delta$ is correct), or one can introduce an effective Hamiltonian,

$$H_{\mathrm{eff}} = H - T\kappa \sum_{n=1}^{N} \ln R_n \tag{6}$$

with $\kappa \equiv 1$ and work directly with a uniform measure for R_n. The incorrect omission of the Jacobian in (5) is equivalent to setting $\kappa = 0$. It is well known [11] that the nodes $R_n = 0$ correspond to core regions of vortices in the dual formulation of the model. The Jacobian factor R (or equivalently the term $-\sum \ln R_n$ in H_{eff}) tends to suppress field configurations with many nodes $R_n = 0$. If the R-factor is omitted, the number of nodes and hence vortices is relatively enhanced. It is thus at least qualitatively plausible that in this case a discontinuous, first-order "freezing

[1]) There is another difference between our update and the update described in the papers [5,8], namely that we do *not* restrict the modulus of the field to a finite interval. This can cause further systematic deviations but we explicitly checked that this is unimportant for the main point here.

transition" from a vortex dominated phase can occur, as is suggested by a similar mechanism for the XY model [11, 13, 14] and defect-models of melting [15, 16].

To be precise we always worked with the proper functional measure in Eq. (5) and replaced the standard Hamiltonian H by [10]

$$H_{\rm gen} = H + T(1-\kappa)\sum_{n=1}^{N} \ln R_n = H + T\delta \sum_{n=1}^{N} \ln |\psi_n| \,, \tag{7}$$

where we have introduced the parameter $\delta = 1 - \kappa$, such that $\delta = 0$ ($\kappa = 1$) corresponds to the standard model and $\delta = 1$ ($\kappa = 0$) to the previously studied modified model with its first-order phase transition for small enough σ.

In the limit of a large parameter σ, it is easy to read off from Eq. (3) that the modulus of the field is squeezed onto unity and once hence expects that irrespectively of the value of κ the XY model limit is approached with its well-known continuous phase transition at $T_c \approx 2.2$. While for the standard model with $\kappa = 1$, this behavior should qualitatively persist for all values of σ, from the numerical results discussed above one expects that for $\kappa = 0$ the order of the transition turns first-order below a certain (tricritical) σ-value. The purpose of this paper is to elucidate this behavior further by studying the phase diagram in the (σ–κ)-plane, i.e. by considering an interpolating model with $\kappa = 1 - \delta$ varying continuously between 0 and 1.

In order to map out the phase diagram in the (σ–κ)- respectively (σ–δ)-plane, we have measured in our Monte Carlo simulations among other quantities the energy density $e = \langle H \rangle / N$, the specific heat per site $c_v = \left(\langle H^2 \rangle - \langle H \rangle^2 \right) / N$, and in particular the mean-square amplitude

$$\langle |\psi|^2 \rangle = \frac{1}{N} \sum_{n=1}^{N} \langle |\psi_n|^2 \rangle \,, \tag{8}$$

which will serve as the most relevant quantity for comparison with previous work [4–8]. For further comparison and as a suitable quantity for locating the critical temperature, we recorded the helicity modulus,

$$\begin{aligned} \Gamma_\mu = \frac{1}{N} \Big\langle \sum_{n=1}^{N} |\psi_n||\psi_{n+\mu}| \cos(\phi_n - \phi_{n+\mu}) \Big\rangle - \\ - \frac{1}{NT} \left\langle \left[\sum_{n=1}^{N} |\psi_n||\psi_{n+\mu}| \sin(\phi_n - \phi_{n+\mu}) \right]^2 \right\rangle , \end{aligned} \tag{9}$$

which is a direct measure of the phase correlations in the μ-direction. Because of cubic symmetry all directions μ are equivalent, and we always quote the average $\Gamma = (1/d) \sum_{\mu=1}^{d} \Gamma_\mu$. In the infinite-volume limit, Γ is zero above T_c and different from zero below T_c. In addition we also measured the density of vortex lines,

$$v = \frac{1}{N} \sum_{x,i} |{*l_{i,x}}| \,. \tag{10}$$

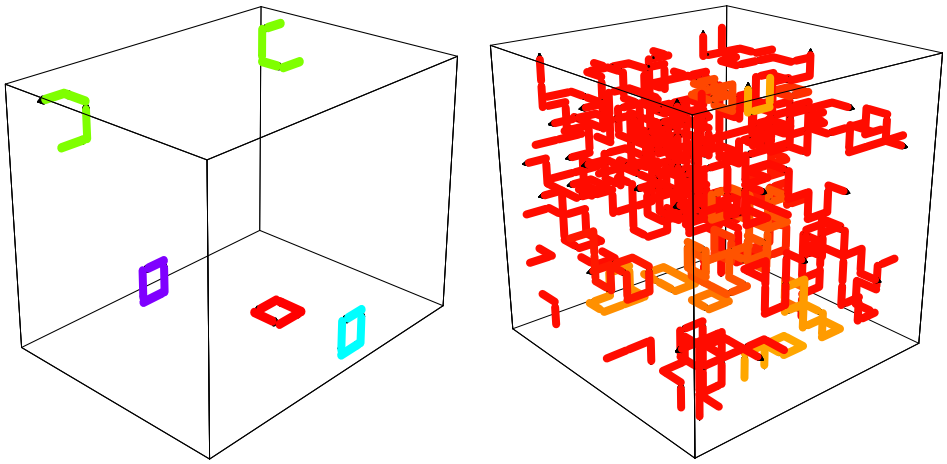

Fig. 3. Networks of closed vortex lines for $\kappa = 1.0$ and $\sigma = 1.0$ in the ordered phase at $T = 0.7$ (left) and disordered phase at $T = 1.4$ (right).

The standard procedure to calculate the vorticity on each plaquette is by considering the quantity

$$m = \frac{1}{2\pi}\big([\phi_1 - \phi_2]_{2\pi} + [\phi_2 - \phi_3]_{2\pi} + [\phi_3 - \phi_4]_{2\pi} + [\phi_4 - \phi_1]_{2\pi}\big)\,,$$

where $\phi_1, \ldots, \phi_4$ are the phases at the corners of a plaquette labeled, say, according to the right-hand rule, and $[\alpha]_{2\pi}$ stands for α modulo 2π: $[\alpha]_{2\pi} = \alpha + 2\pi n$, with n an integer such that $\alpha + 2\pi n \in (-\pi, \pi]$, hence $m = n_{12} + n_{23} + n_{34} + n_{41}$. If $m \neq 0$, there exists a vortex which is assigned to the object dual to the given plaquette, i.e. a link in three dimensions. Hence, the topological charges are represented by (oriented) line elements $*l_i$ (which can take three values: 0, ± 1; the values ± 2 have a negligible probability) and combine to form closed networks ("vortex loops"). Example plots in the ordered and disordered phase, respectively, are shown in Fig. 3, and a detailed discussion of their behavior with special emphasis on percolation properties is given in Ref. [17].

We further analyzed the Binder cumulant,

$$U = \frac{\langle(\vec{\mu}^2)^2\rangle}{\langle\vec{\mu}^2\rangle^2}\,,$$

where $\vec{\mu} = (\mu_x, \mu_y)$ with

$$\mu_x = \frac{1}{N}\sum_{n=1}^{N} \mathrm{Re}(\psi_n)\,, \quad \mu_y = \frac{1}{N}\sum_{n=1}^{N} \mathrm{Im}(\psi_n)\,,$$

is the magnetization per lattice site of a given configuration.

3 Monte Carlo simulations

A safe (but inefficient) method for simulating the complex measure (5) is provided by the standard Metropolis algorithm [18], where the field ψ_n is decomposed into its Cartesian components, $\psi_n = \psi_{x,n} + \mathrm{i}\psi_{y,n}$. For each lattice site a random update proposal for the two components is made, e.g. $\psi_{x,n} \to \psi_{x,n} + \delta\psi_{x,n}$ with $\delta\psi_{x,n} \in [-\Delta, \Delta]$, and in the standard fashion accepted or rejected according to the energy change δH_{gen}. The well-known drawback of this algorithm is its severe critical slowing down (large autocorrelation times) in the vicinity of a continuous phase transition [19], leading to large statistical errors for a fixed computer budget. To improve the accuracy of our data we therefore employed the single-cluster algorithm [20] to update the direction of the field [21], similar to simulations of the XY spin model [22]. The modulus of ψ is updated again with a Metropolis algorithm. Here some care is necessary to treat the measure (5) properly (see above comments). Per measurement we performed one sweep with the Metropolis algorithm and n single-cluster updates. In all simulations the number of cluster updates was chosen such that $n\langle|C|\rangle \approx L^d \equiv N$, where $\langle|C|\rangle$ is the average cluster size. Since $\langle|C|\rangle$ scales with system size as the susceptibility, $\chi = N\langle\vec{\mu}^2\rangle \simeq L^{\gamma/\nu}$ with $\gamma/\nu = 2 - \eta \approx 2$, n was chosen $\propto L$. For each simulation point we first thermalized with 500 to 1 000 sweeps and then averaged over 10 000 measurements. In the following we only show the more extensive and accurate data set of the cluster simulations, but we tested in many representative cases that they coincide with the Metropolis simulations within error bars, which are always computed with the Jackknife method [23].

In the cases of strong first-order phase transitions (for the non-generic case $\kappa = 0$) also cluster simulations become inefficient. To bypass this problem we employed here a variant of the multicanonical scheme [24] where the histogram of the mean modulus is flattened instead that of the energy ("multimodulus" simulations). With this simulation technique we overcome the difficulty of sampling the extremely rare events between the two peaks of the canonical distribution [25].

4 Results

To substantiate our claim we first concentrated on the two most characteristic cases $\kappa = 0$ and $\kappa = 1$ for a small value of the parameter $\sigma = 0.25$. For $\kappa = 0$, we observe already on very small lattices a clear double-peak structure for the distributions of the energy and mean-square amplitude as well as the mean modulus

$$\overline{|\psi|} = \frac{1}{N}\sum_{n=1}^{N}|\psi_n|$$

depicted in Fig. 4. Notice that already for the extremely small lattice size of 4^3 the minimum between the two peaks is suppressed by more than 20 orders of magnitude. This is an unambiguous sign for two coexisting phases and thus clearly implies that the model undergoes a first-order phase transition in the small σ-regime for $\kappa = 0$.

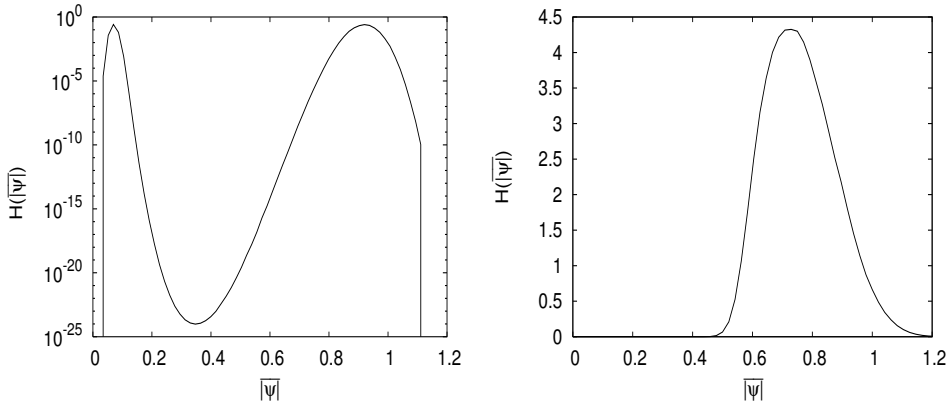

Fig. 4. Left: Histogram of the mean modulus $\overline{|\psi|}$ for $\kappa = 0$ and $\sigma = 0.25$ on a logarithmic scale for a 4^3 cubic lattice, reweighted to the temperature $T_0 \approx 0.0572$ where the two peaks are of equal height. Right: Histogram for the same quantity and lattice size for $\kappa = 1$ and $\sigma = 0.25$ at $T = 1.1$ close to the second-order phase transition point.

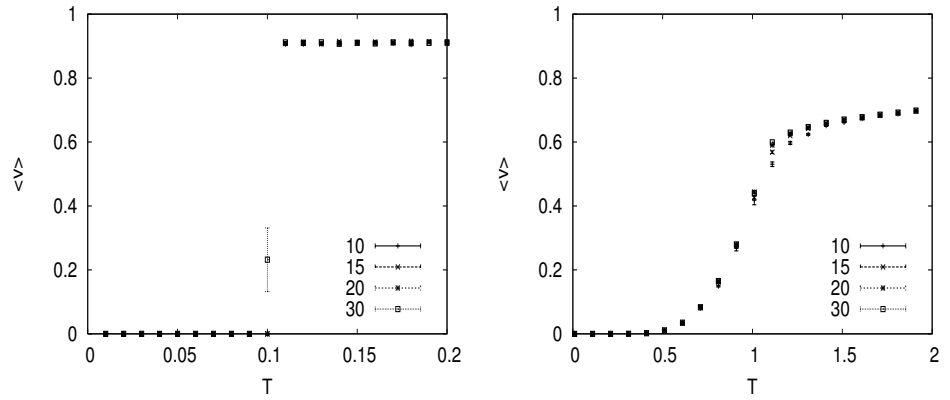

Fig. 5. Vortex-line density for $\kappa = 0$ (left) and $\kappa = 1$ (right) at $\sigma = 0.25$.

For the standard model with $\kappa = 1$, on the other hand, we observe for *all* σ-values a smooth behavior, suggesting that the XY model like continuous transition for $\sigma \to \infty$ persists also for small σ-values. This is clearly supported by the single-peak structure of all distributions just mentioned; for the case of the mean modulus see the right plot of Fig. 4. These findings are also clearly reflected in the topological excitations of the model. The vortex-line density depicted in Fig. 5 shows for $\kappa = 0$ a pronounced jump, typical for a first-order phase transition, while for $\kappa = 1$ it varies smoothly across the transition point. The κ-dependence is illustrated in Figs. 6 and 7, indicating that for $\sigma = 0.25$ the cross-over from first- to second-order phase transitions takes place between $\kappa = 0.8$ and 0.9.

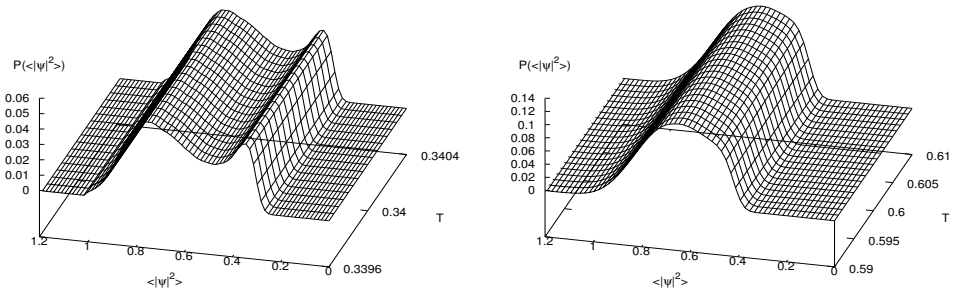

Fig. 6. Histograms of the squared modulus for $\sigma = 0.25$ and $\kappa = 0.8$ (left) resp. $\kappa = 0.9$ (right) on a 4^3 cubic lattice.

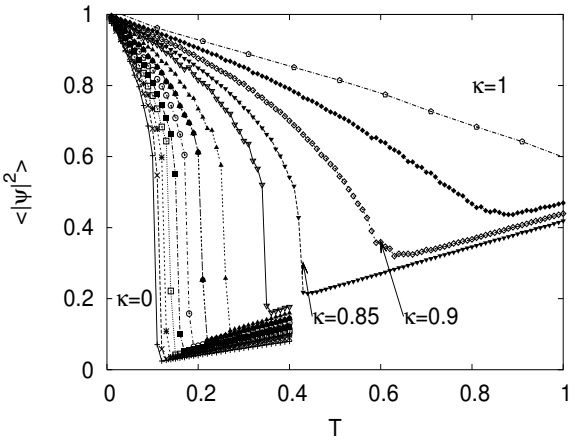

Fig. 7. The κ dependence of the mean-square amplitude $\langle|\psi|^2\rangle$ as a function of temperature on a 15^3 lattice for $\sigma = 0.25$.

To exemplify the big differences between the models with $\kappa = 0$ and $\kappa = 1$, we choose in the following the case $\sigma = 1.5$ and present careful finite-size scaling (FSS) analyses. We begin with the non-standard case $\kappa = 0$, where the first-order phase transition around $T \approx 0.36$ is still pronounced but much less strong than for $\sigma = 0.25$. Still, in order to get sufficiently accurate equilibrium results, the simulations for lattices of size $L = 4$, 6, 8, 10, 12, 14, 15 and 16 had to be performed again with our multimodulus simulation method. In fact, as can be inspected in the histogram plots for the mean modulus shown in Fig. 8, the frequency of the rare events between the two peaks in the canonical ensemble for a 16^3 lattice is about 50 orders of magnitude smaller than for configurations contributing to the two peaks.

The strength of the transition can be characterized more quantitatively by es-

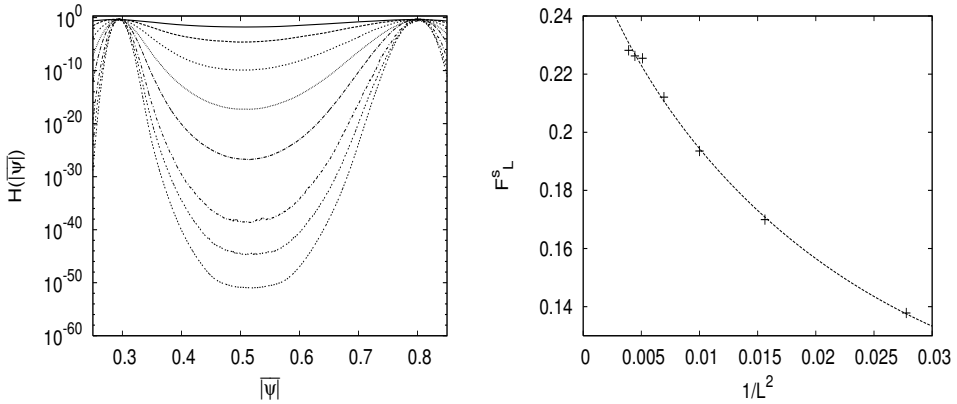

Fig. 8. Left: Histogram of the mean modulus $\overline{|\psi|}$ for $\kappa = 0$ and $\sigma = 1.5$ on a logarithmic scale for various lattice sizes ranging from $L = 4$ (top curve) to $L = 16$ (bottom curve), reweighted to temperatures where the two peaks are of equal height. Right: FSS extrapolation for $L \geq 6$ of the interface tension F_L^s, yielding the infinite-volume limit $F^s = 0.271(5)$.

timating the interface tension [25],

$$F_L^s = \frac{1}{2L^{d-1}} \ln \frac{P_L^{\max}}{P_L^{\min}} ,$$

where $P_L^{\max}$ is the value of the two peaks and $P_L^{\min}$ denotes the minimum in between. Here we have assumed that for each lattice size the temperature was chosen such that the two peaks are of equal height which can be achieved by histogram reweighting. The thus defined temperatures approach the infinite-volume transition temperature as $1/L^d$, and for the final estimate of $F^s = \lim_{L\to\infty} F_L^s$, we performed a FSS fit according to [26]

$$F_L^s = F^s + \frac{a}{L^{d-1}} + \frac{b \ln L}{L^{d-1}} . \tag{11}$$

As is shown in Fig. 8, the finite-lattice estimates F_L^s are clearly nonzero and the infinite-volume extrapolation (11) tends to increase with system size, yielding a comparably large interface tension of $F^s = 0.271(5)$.

In the generic case $\kappa = 1$, the model with $\sigma = 1.5$ definitely exhibits a continuous phase transition around $\beta \equiv 1/T \approx 0.8$. To confirm the expected critical exponents of the O(2) or XY model universality class, we simulated here close to criticality somewhat larger lattices of size $L = 4$, 8, 12, 16, 20, 24, 32, 40 and 48 and performed a standard FSS analysis. From short runs we first estimated the location of the phase transition to be at $\beta_0 = 0.7795 \approx \beta_c$. In the long runs at β_0 we recorded the time series of the energy density $e = E/N$, the magnetization $\vec{\mu}$, the mean modulus $\overline{|\psi|}$, and the mean-square amplitude[2]) $|\psi|^2$, as well as the helicity modulus Γ_μ and

[2]) Recall that $\overline{|\psi|} \equiv \sum_{n=1}^N |\psi_n|/N$ and $|\psi|^2 \equiv \sum_{n=1}^N |\psi_n|^2/N$, such that $\overline{|\psi|}^2 \neq |\psi|^2$.

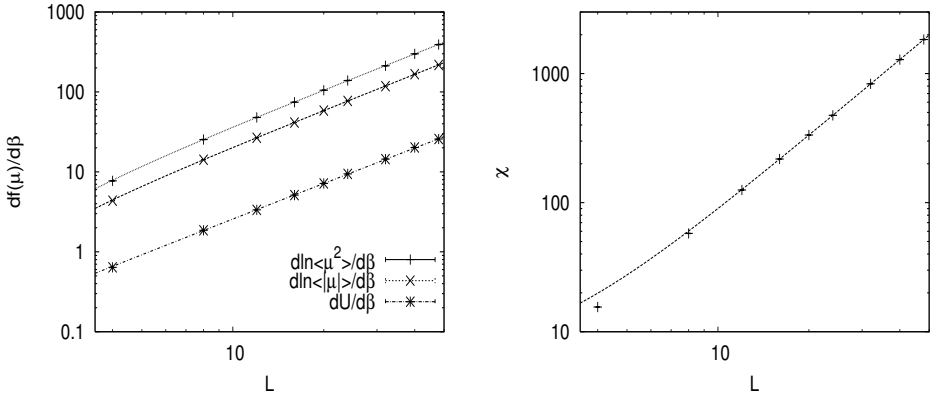

Fig. 9. FSS behavior for $\kappa = 1$ and $\sigma = 1.5$. Left: Least-square fits on a log–log scale, using the FSS ansatz $\mathrm{d}f(\mu)/\mathrm{d}\beta \propto L^{1/\nu}$ at the maxima locations. The fits using the data for $L \geq 8$ lead to an overall critical exponent $1/\nu = 1.493(7)$ or $\nu = 0.670(3)$. Right: Log–log plot of the FSS of the susceptibility at $\beta = 0.780\,08 \approx \beta_c$. The line shows the three-parameter fit $a + bL^{\gamma/\nu}$, yielding for $L \geq 16$ the estimate $\gamma/\nu = 1.962(12)$.

the vorticity v. After an initial equilibration time, we took here about 1 000 000 measurements for each lattice size. Applying the reweighting technique we first determined the maxima of the susceptibility, $\chi' = N(\langle\vec{\mu}^2\rangle - \langle|\vec{\mu}|\rangle^2)$, of $\mathrm{d}\langle|\vec{\mu}|\rangle/\mathrm{d}\beta$, and of the logarithmic derivatives $\mathrm{d}\ln\langle|\vec{\mu}|\rangle/\mathrm{d}\beta$ and $\mathrm{d}\ln\langle\vec{\mu}^2\rangle/\mathrm{d}\beta$. The locations of these maxima provide us with four sequences of pseudo-transition points $\beta_{\max}(L)$ for which the scaling variable $x = (\beta_{\max}(L) - \beta_c)L^{1/\nu}$ should be constant. Using this fact we then have several possibilities to extract the critical exponent ν from (linear) least-squares fits of the FSS ansatz $\mathrm{d}U/\mathrm{d}\beta \cong L^{1/\nu} f_0(x)$ or $\mathrm{d}\ln\langle|\vec{\mu}|^p\rangle/\mathrm{d}\beta \cong L^{1/\nu} f_p(x)$ to the data at the various $\beta_{\max}(L)$ sequences. The quality of our data and the fits starting at $L_{\min} = 8$, with goodness-of-fit parameters $Q = 0.85$ – 0.90, can be inspected in Fig. 9. All resulting exponent estimates, and consequently also their weighted average

$$\frac{1}{\nu} = 1.493(7)\,, \quad \nu = 0.670(3)\,,$$

are in perfect agreement with recent high-precision Monte Carlo estimates for the XY model universality class [21, 27]. Note that hyperscaling implies $\alpha = 2 - 3\nu = -0.010(9)$, which also favorably compares with recent spacelab experiments on the lambda transition in liquid helium [28].

Assuming thus $1/\nu = 1.493$ we can improve our estimate for β_c from linear least-squares fits to the scaling behavior of the various $\beta_{\max}$ sequences. The combined estimate from the four sequences is $\beta_c = 0.780\,08(4)$. To extract the critical exponent ratio γ/ν we can now use the scaling relation for the susceptibility $\chi = N\langle\vec{\mu}^2\rangle \simeq a + bL^{\gamma/\nu}$ at β_c. For $L \geq 16$ we obtain from the FSS fit with $Q = 0.70$

shown on the r.h.s. of Fig. 9 the estimate of

$$\frac{\gamma}{\nu} = 1.962(12)[9]\,,$$

where we also take into account the uncertainty in our estimate of β_c; this error is estimated by repeating the fit at $\beta_c \pm \Delta\beta_c$ and indicated by the number in square brackets. Here we find a slight dependence of this value on the lower bound of the fit range $[L_{\min}, 48]$, i.e., one would have to include larger lattices for a high-precision estimate of the critical exponent ratio γ/ν, but this was not our objective here. Still, these results are in good agreement with recent high-precision estimates in the literature [21, 27] and clearly confirm the expected second-order nature of the phase transition in the standard complex $|\psi|^4$ model, governed by XY model critical exponents.

A similar set of simulations at $\sigma = 0.25$ for lattice sizes $L = 4$, 8, 12, 14, 16, 20, 24, 28, 32 and 40 gave the exponent estimates $1/\nu = 1.498(9)$, $\nu = 0.668(4)$ and $\gamma/\nu = 1.918(71)[8]$ (at $\beta_c = 0.9284(4)$), which are less accurate but again compatible with the XY model universality class. At any rate these results definitely rule out the possibility of a first-order phase transition in the standard model at small σ-values. When going to even smaller σ-values, the FSS analysis is more and more severely hampered by the vicinity of the Gaussian fixed point which induces strong crossover scaling effects. Since consequently very large system sizes would be required to see the true, asymptotic (XY model like) critical behavior we have not further pursued our attempts in this direction. Here we only add the remark that for $\sigma = 0.01$ the energy and magnetization distributions exhibit a clear single-peak structure for all considered lattice sizes up to $L = 20$, showing that in the standard model with $\kappa = 1$ a phase-fluctuation induced first-order phase transition is very unlikely even for very small σ values.

For the non-generic case $\kappa = 0$, a look back at Fig. 2 shows that the crossover from first- to second-order transitions happens around $\sigma_t \approx 2.5$. The resulting transition lines in the (σ–T)-plane for $\kappa = 0$ and $\kappa = 1$ are sketched on the l.h.s. of Fig. 10, with the thick line for $\kappa = 0$ indicating the approximate regime of first-order phase transitions. We also checked the critical behavior along the line of second-order transitions for $\kappa = 0$. Specifically, at $\sigma = 5$, i.e. sufficiently far away from σ_t, we obtained from FSS fits to data for lattices of size $L = 4$, 8, 12, 16, 20, 24, 28, 32 and 40 the exponent estimates $1/\nu = 1.489(7)$, $\nu = 0.671(3)$ and $\gamma/\nu = 1.913(82)[13]$ (at $\beta_c = 0.97253(4)$). As expected by symmetry arguments, also these results for the second-order regime of the $\kappa = 0$ variant of the model are in accord with the XY model universality class.

In a second set of simulations we explored the two-dimensional (σ–κ) parameter space of the generalized Ginzburg–Landau model in the orthogonal direction by performing simulations at fixed σ values and varying κ from 0 to 1. For most σ-values we concentrated on the crossover region between first- and second-order transitions with increasing κ. For two selected values, $\sigma = 0.25$ and $\sigma = 1.5$, we studied the κ dependence more systematically by simulating all values from $\kappa = 0$ to 1 in steps of 0.1. In addition we performed two further runs in the crossover

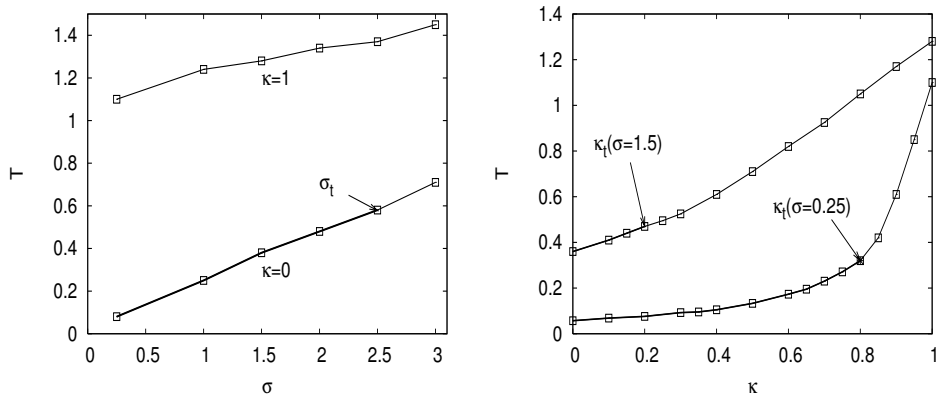

Fig. 10. Left: Transition lines in the (σ–T)-plane for $\kappa = 0$ and $\kappa = 1$. The thick line for $\kappa = 0$ indicates first-order phase transitions while all other transitions are continuous. Right: Phase diagram in the (κ–T)-plane for $\sigma = 0.25$ and $\sigma = 1.5$. The transitions along the thick line for $\kappa < \kappa_t$ are of first order while the transitions for $\kappa > \kappa_t$ are of second (or higher) order. The points labeled σ_t and κ_t at the intersection of the two regimes are tricritical points.

regime at $\kappa = 0.85$ and 0.95 for $\sigma = 0.25$ as well as at $\kappa = 0.15$ and $\kappa = 0.25$ for $\sigma = 1.5$. For example, from Fig. 7 we read off that for $\sigma = 0.25$ the crossover between the two types of phase transitions happens around $\kappa_t(\sigma = 0.25) \approx 0.8$, and the analogous analysis for $\sigma = 1.5$ yields $\kappa_t(\sigma = 1.5) \approx 0.2$. The resulting transition lines for these two σ-values are plotted on the r.h.s. of Fig. 10, where the thick lines indicate again first-order phase transitions.

Finally, by combining all numerical evidences collected so far with additional data not described here in detail, we find the phase structure in the (σ–κ)-plane depicted in Fig. 11. All points in the lower left corner for small σ and small κ exhibit a first-order phase transition when the temperature is varied, while all points in the upper right corner display a continuous transition of the XY model type. This means in particular that for the standard model parametrized by $\kappa = 1$ this is always true. Quantitatively the XY model is reached for all κ-values in the limiting case $\sigma \longrightarrow \infty$.

5 Summary

Our numerical simulations of the standard three-dimensional Ginzburg–Landau model do not support the possibility of phase-fluctuation induced first-order phase transitions as suggested by approximate variational calculations [4]. Rather, down to very small values of the parameter σ, the transitions are found to be continuous, as expected on general grounds. Our results suggest, however, that a generalized Ginzburg–Landau model can be tuned to undergo first-order phase transitions by a mechanism similar to that discussed in Ref. [13] when varying the parameter

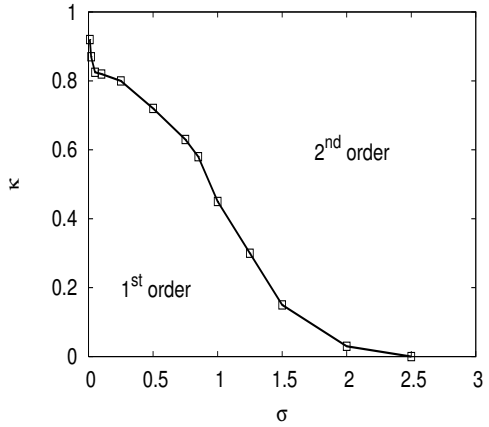

Fig. 11. Phase structure in the (σ–κ)-plane of the generalized complex Ginzburg–Landau model in three dimensions, separating regions with first- and second-order phase transitions, respectively, when the temperature is varied. All continuous transitions fall into the XY model universality class which is approached for all κ-values in the limit $\sigma \longrightarrow \infty$.

κ of an additional $\sum \ln R_n$ term in the generalized Hamiltonian (7). Following Ref. [13] this can be understood by a duality argument. For $0 \leq \kappa < 1$ the extra term reduces the ratio of core energies of vortex lines of vorticity two versus those of vorticity one, and this leads to the same type of transition observed in defect models of crystal melting.

The phase transitions of the standard model as well as the continuous transitions of the generalized model are confirmed to be governed by the critical exponents of the XY model or O(2) universality class, as expected by general symmetry arguments. For the generalized model it would be interesting to analyze in more detail the tricritical points separating the regions with first- and second-order phase transitions. Such a study, however, is quite a challenging project and hence left for future work.

Exploratory simulations of the two-dimensional case [10], where the standard model exhibits Kosterlitz–Thouless transitions, indicate that a similar mechanism can drive the transition of the generalized model to first order also there.

E.B. thanks the EU network HPRN-CT-1999-00161 EUROGRID – "Geometry and Disorder: from membranes to quantum gravity" for a postdoctoral grant. Financial support by the Deutsche Forschungsgemeinschaft (DFG) under grant No. JA483/17-3 and the German-Israel-Foundation (GIF) under contract No. I-653-181.14/1999 is also gratefully acknowledged.

References

[1] J. Zinn-Justin: *Quantum Field Theory and Critical Phenomena*. 3rd ed., Clarendon Press, Oxford, 1996.

[2] H. Kleinert and V. Schulte-Frohlinde: *Critical Properties of Φ^4-Theories*. World Scientific, Singapore, 2001.

[3] H. Kleinert: Phys. Rev. Lett. **84** (2000) 286.

[4] P. Curty and H. Beck: Phys. Rev. Lett. **85** (2000) 796.

[5] P. Curty and H. Beck: e-print `cond-mat/0010084`.

[6] H. Fort: e-print `hep-th/0010070`.

[7] G. Alvarez and H. Fort: Phys. Rev. B **63** (2001) 132504; Phys. Lett. A **282** (2001) 399.

[8] G. Alvarez and H. Fort: Phys. Rev. B **64** (2001) 092506.

[9] E. Bittner and W. Janke: Phys. Rev. Lett. **89** (2002) 130201.

[10] E. Bittner and W. Janke: Phys. Rev. B **71** (2005) 024512.

[11] H. Kleinert: *Gauge Fields in Condensed Matter*. Vol. I: *Superflow and Vortex Lines*. World Scientific, Singapore, 1989.

[12] V.M. Loktev, R.M. Quick and S.G. Sharapov: Phys. Rep. **349** (2001) 1.

[13] W. Janke and H. Kleinert: Nucl. Phys. B **270** (1986) 399.

[14] P. Minnhagen and M. Wallin: Phys. Rev. B **36** (1987) 5620;
G.-M. Zhang, H. Chen and X. Wu: Phys. Rev. B **48** (1993) 12304;
D. Yu. Irz, V.N. Ryzhov and E.E. Tareyeva: Phys. Rev. B **54** (1996) 3051.

[15] H. Kleinert: *Gauge Fields in Condensed Matter*. Vol. II: *Stresses and Defects*. World Scientific, Singapore, 1989.

[16] W. Janke: Int. J. Theor. Phys. **29** (1990) 1251.

[17] E. Bittner, A. Krinner and W. Janke: Phys. Rev. B **72** (2005) 094511.

[18] N. Metropolis, A.W. Rosenbluth, M.N. Rosenbluth, A.H. Teller and E. Teller: J. Chem. Phys. **21** (1953) 1087.

[19] W. Janke: Mathematics and Computers in Simulations **47** (1998) 329; and in *Computational Physics: Selected Methods – Simple Exercises – Serious Applications*. Eds. K.H. Hoffmann and M. Schreiber, Springer, Berlin, 1996, p. 10.

[20] U. Wolff: Phys. Rev. Lett. **62** (1989) 361; Nucl. Phys. B **322** (1989) 759.

[21] M. Hasenbusch and T. Török: J. Phys. A **32** (1999) 6361.

[22] W. Janke: Phys. Lett. A **148** (1990) 306.

[23] B. Efron: *The Jackknife, the Bootstrap and Other Resampling Plans*. Society for Industrial and Applied Mathematics SIAM, Philadelphia, 1982.

[24] B.A. Berg and T. Neuhaus: Phys. Lett. B **267** (1991) 249; Phys. Rev. Lett. **68** (1992) 9.

[25] W. Janke: in *Computer Simulations of Surfaces and Interfaces*, NATO Science Series, II. Mathematics, Physics and Chemistry – Vol. **114**, Proceedings of the NATO Advanced Study Institute, Albena, Bulgaria, 9–20 September 2002. Eds. B. Dünweg, D.P. Landau, and A.I. Milchev, Kluwer, Dordrecht, 2003, pp. 111–135.

[26] U. Hansmann, B.A. Berg and T. Neuhaus: Int. J. Mod. Phys. C **3** (1992) 1155.

[27] M. Campostrini, M. Hasenbusch, A. Pelissetto, P. Rossi and E. Vicari: Phys. Rev. B **63** (2001) 214503.

[28] J.A. Lipa, J.A. Nissen, D.A. Stricker, D.R. Swanson and T.C.P. Chui: Phys. Rev. B **68** (2003) 174518.